IJSMDO

RESEARCH ARTICLE

OPEN ACCESS

The fluidic molecular trajectory and the Nano-droplet production ability

Van Quang Nguyen[1*], Van Thien Nguyen[2], Tien Dung Hoang[1], Pham Thi Minh Hue[1], Nguyen Chi Tam[1], Le Thi Phuong Thanh[1], and Ta Thi Tra Giang[1]

[1] School of Mechanical and Automotive Engineering, Ha Noi University of Industry, No 298, Cau Dien Street, Bac Tu Liem District, Hanoi City, Vietnam

[2] Personnel and Administration Department, Ha Noi University of Industry, No 298, Cau Dien Street, Bac Tu Liem District, Hanoi City, Vietnam

Abstract. This paper studies the liquid Nano-droplet production ability using molecular dynamics simulation methodology. The research parameter is performed at the temperature of 310 Kelvin (K), the pressing force of 10.0×10^{-10} Newton (N) and the ejective hole diameters of 25 and 40 Angstrom (Å). The research result shows that liquid Nano-droplets finally were not produced for the ejective diameter of 25 Å. The Nano-jets were not only non-destruction from nozzle's surface to produce the droplets but also movement downward to come back the nozzle's surface. The molecular trajectory is very zigzag and curved both inside and outside the ejective container. In the contrary, when increasing the ejective diameter to 40 Å, the liquid Nano-droplet was produced in the same the ejective time and compressible force magnitude. The molecular trajectory is quite straight after ejecting out the outside of the container. Meanwhile, for the nozzle diameter size of 40 Å, the Nano-droplet was not only production but also movement up to leave away the nozzle's surface under same above conditions. That proves that the ejective diameter has the influences to the moveable direction and Nano-droplets formation ability in the whole ejective process.

Keywords: Fluidic molecular trajectory / fluidic nano-droplets / molecular dynamics methodology / nozzle diameter size

1 Introduction

The Nano-fluidic technology is used very popular in many fields industrial applications such print technology, cooling and lubrication systems in metallic machining, the electrical circuit board and printed circuit board manufacturing, and many more. In the Nano-fluidic ejection process, the requirement about the parameter optimization and choice for manufacturing the ejective device and ejection process always plays an important problem to improve the features of ejective device.

The molecular dynamics (MD) simulation is an important method which is adopted to investigate the physics of Nano-scale ejection systems. The MD method has adopted to simulate for propane molecular ejection with nozzle orifice diameters between 2 and 6 nm.

Otherwise, the parameter about the viscosity, wetting, and nozzle configuration factor which affect to the jet formation was also discussed [1].

The finding about the separation criteria of nanoscale water droplets [2], method also adopted to simulate the ejection and the formation of Nano-scale fluidic droplets [3]. The parameter about the nozzle diameter, pressing force and system temperature magnitudes [4], fluidic flow dynamics which affect to the jet formation, the formation of liquid sheets by deposition of droplets on a surface [5], the novel approach for using an efficient optimization technique was investigated [6].

The molecular dynamics method was also used to nanoscale friction behavior and deformation [7], the role of thermal fluctuations on the formation and stability of nano-scale drops [8], establish the water Nano-jet and Nano-droplet formation ability [9,10]. A combination of the Lenard-Jones and Coulomb potentials about interacting between the water charge and metal molecular distributions is used for the interaction on the ejective device's wall [11,12].

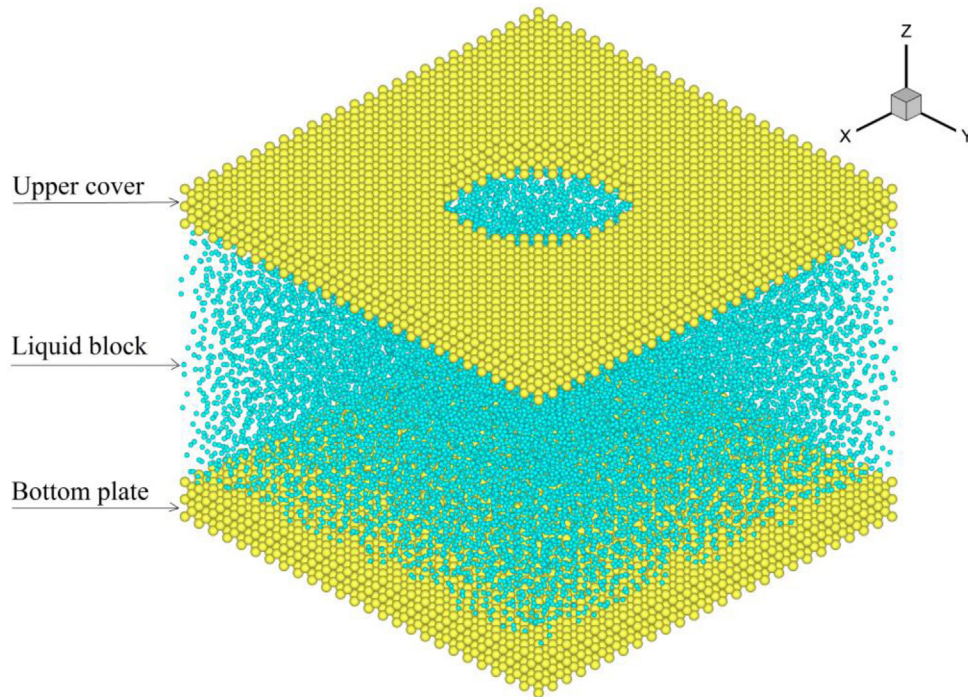*e-mail: nguyenvanquang@haui.edu.vn;
nguyenquang.kuas@gmail.com

Fig. 1. Fluid molecular simulation model.

The effects of temperature and aperture size parameters on the liquid ejection process by using molecular dynamics simulation were performed [13]. According to the analysis, the Nano-jet aperture is distributed as the temperature is increased under these effects [14]. The fluidic-droplet formation behavior was also investigated with two fluid types of water and ethylene glycol [15,16]. Otherwise, the effects of pressing force, temperature system and nozzle size parameter on the liquid ejection process by using molecular dynamics method and the positive voltage keeping time, pulse voltage magnitude on the fluidic droplet size and velocity were investigated [17,18].

Many scientists have mentioned to the simulation and experimental studies of the fluidic molecular ejection process by molecular dynamics methodology. However, the investigation about effect of the parameter on the ejection process of the fluidic molecule and Nano-jet formation has rarely been performed. This research is a continuation of a previous study [20] using MD simulation methods to survey the fluidic molecular trajectory and the Nano-droplet production ability and the causes which affect to these problems are discussed.

2 Research methodology

2.1 Molecular simulation model

The position of model parts is arranged as in Figure 1. The x- and y-directions along to the container were used to set up the periodic boundary conditions to limit the movement of molecules. The fluid molecules are contained in the space among the periodic boundary conditions, nozzle and back plates. The distance is 60.872 Å from the nozzle to back

plate. The container is a cubic shape with all dimensions of 101.9 Å along both the x-, and y-axis directions. The container contains 20 691 fluid molecules inside with the molecular density of 0.999972 g/cm^3.

The nozzle and back plates are composed of gold (Au) atoms and arranged into the crystal lattice structures of face-centered cubic (FCC) with the lattice constant a = 4.076 Å. The nozzle plate at the highest position is fixed while the back plate at the lowest position can move vertically under a pressing force on the back plate in the $+z$-direction. The nozzle and back plates both include 5 layers of gold atom which have the thickness of 8.152 Å. The back plate has total 6 503 atoms. The nozzle plate has an aperture in the center with number of atoms are 6 200, 5 924, and 5 772 for the 25- and 40-Å-diameter nozzle apertures, respectively.

LAMMPS software and C++ code were used as the tools for performing the simulation and analysis the results in this research.

2.2 Molecular interaction

The molecules have the structure of the flexible three-centered (F_3C) which was used to study by the molecular dynamic simulation method. The interaction among the atoms is evaluated the specific potential model and the shifted Lenard-Jones 12-6 potential. The vibration of the molecules is evaluated Harmonic potential function. The molecular equilibrium values are the bond length and angle of respectively 1.0 Å and 104.5 degrees.

The molecular energy function [21] was employed to present the Coulomb terms and sum of the bonding, bending and the van der Waals which can be expressed as equation (1):

Table 1. Simulation scheme.

Case	Nozzle hole diameter (Å)	Temperature (K)	Pressing force (N)
1	25	310	10.0×10^{-10}
2	25	310	12.0×10^{-10}
3	40	310	10.0×10^{-10}
4	40	310	12.0×10^{-10}

$$U = U_{bond} + U_{bend} + U_{vdw} + U_{els}$$

$$= \sum K_b^{OH}(r_i - r_{eq})^2 + \sum K_\theta^{HOH}(\theta_i - \theta_{eq})^2$$
$$+ \sum \left[A_{SC}\varepsilon_{ij}\left(\frac{r_0^{ij}}{r_{ij}}\right)^{12} - 2\varepsilon_{ij}\left(\frac{r_0^{ij}}{r_{ij}}\right)^6 - S_{vdw}(r_{ij}) \right]$$
$$+ \sum \left[\frac{q^i q^j}{r_{ij}} - S_{els}(r_{ij}) \right], \tag{1}$$

In there, $S_{vdw}(r_{ij})$ is the truncation shift function of the van der Waals force as equation (2):

$$S_{vdw}(r_{ij}) = \left\{ U_r - U_{r_c} - (r - r_c)\left(\frac{dU}{dr}\right)_{r_c} \text{for} \, r < r_c 0 \, \text{for} \, r \geq r_c, \right. \tag{2}$$

and $S_{eis}(r_{ij})$ is the shift function for the Coulomb's force as equation (3):

$$S_{els}(r_{ij}) = (r - r_c)\left[\frac{q^i q^j}{r_c^2}\right], \tag{3}$$

In there, $A_{sc}, K_b^{OH}, K_\theta^{OH}, r_i, r_{eq}, \theta_i, \theta_{eq}, r_{ij}$ and r_c are the coefficients for adjusting the short distance force, the harmonic force constant, the angle bending force constant, the i th O-H bond length, the equilibrium length of the O-H bond, the i th H-O-H bond angle, the equilibrium angle of the H-O-H bond angle, the interatomic distance, and the cutoff distance (10 Å), respectively. Terms q_i and q_j are the partial charges of O or H.

The interactions between the water molecules and the gold atoms are represented by the Spohr potential functions of

$$U_{Au-H_2O} = U_{Au-O}(r_{Au-O}) + U_{Au-H_1}(r_{Au-H_1}) + U_{Au-H_2}(r_{Au-H_2}), \tag{4}$$

with

$$U_{Au-O}(r) = S_2(r)D_0[\exp(-2\alpha_0(r - r_{e1})) - 2\exp(-\alpha_0(r - r_{e1}))], \tag{5}$$

and

$$U_{Au-H}(r) = \gamma D_0 \exp\left(-2\alpha_H(r - r_{e2})\right). \tag{6}$$

The switch function $S_2(r)$ has the form of

$$S_2(r) = \begin{cases} 1 \text{for} \, r \leq r_{on} \\ \dfrac{(r_{off}^2 - r^2)^2(r_{off}^2 + 2r^2 - 3r_{on}^2)}{(r_{off}^2 - r_{on}^2)^3} \text{for} \, r_{on} < r < r_{off} \end{cases}, \tag{7}$$

where r_{on} and o_{ff} are the start and end distances of the switch function which respectively have the values 7.0 and 11.0 Å.

2.3 Simulation scheme

This study performs four simulation cases for two sizes of ejective aperture diameters 25 and 40-Å as shown in Table 1. The temperature of 310 K is adopted to reach an equilibrium state for the fluid molecule inside the ejective system. The pressing force magnitudes are 10.0×10^{-10} and 12.0×10^{-10} (N) which were used to press on the back plate to push the fluid molecules out of the nozzle aperture.

The data output frequency is once per 5000 time steps for the total simulation length in each scheme is 200 000 time steps with the cases as listed in Table 1.

3 Research result and discussion

3.1 Fluid molecule ejection result through various nozzle apertures

Snapshots of the fluidic Nano-jet corresponding to different nozzle hole diameters of 25- and 40-Å at 150 000 fs are shown in Figure 2. Figures 2a-d Figures 2a-d respectively show the snapshots of the fluidic Nano-jet ejected out through 25 and 40-Å-diameter nozzle under the same system temperature and various pressing forces. In these cases, the fluidic Nano-jets did not separate from the nozzle plate surface and form a Nano-scale fluid droplet for 25-Å-diameter nozzle. In contract, the snapshots of the Nano-scale fluid jets ejected through 40-Å-diameter nozzle apertures with the same condition of temperature and pressing force. The droplets were separated out from the jets to form the Nano-scale fluid droplets for these cases at 150 000 fs.

The snapshots of the fluidic Nano-jet in Figure 2 show that the diameter of the nozzle aperture has affected to the separated ability of the fluid Nano-jet. To investigate about
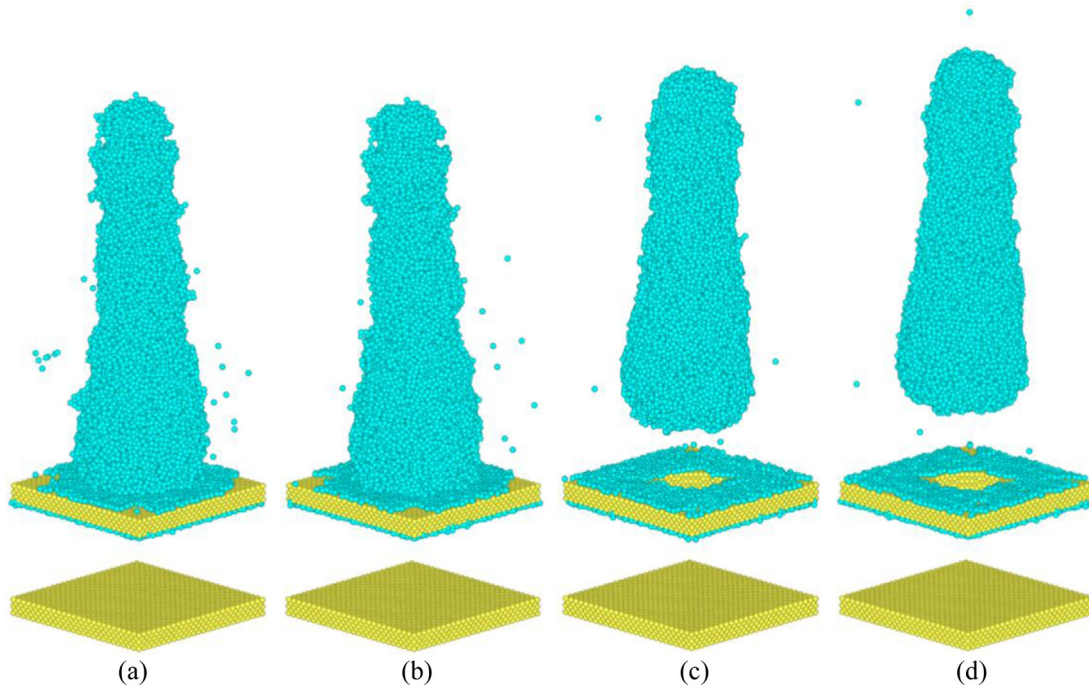
Fig. 2. Snapshots of the fluidic Nano-jet at 150 000 fs: (a) and (b) fluidic Nano-jets of 25-Å-diameter nozzle; (a) and (b) fluidic Nano-jets of 40-Å-diameter nozzle.

this problem, Author performs to study two typically 25 and 40-Å-diameter nozzles under the same system temperature of 310 (K) and various pressing forces of 10.0×10^{-10} and 12.0×10^{-10} (N). The fluidic molecule trajectory is used to analyze and explain for the Nano-droplet production ability with two above typically nozzle diameters.

When the simulation process continues to perform for increasing the simulation time from 150 000 fs to 200 000 fs, the results show that the fluidic Nano-jets still didn't separate out from the nozzle plate and form a Nano-scale fluid droplet for 25-Å-diameter nozzle as shown in Figures 3a and 3b. Two these jets are not only the fluid jets are not only non-continuous to move up but also moving back to the nozzle plate's surface when increasing the simulation time to 200 000 fs. Contrarily, the Nano-scale fluid droplets were produced from the Nano-jets when they continue movement up to leave away the nozzle plate for 40-Å-diameter nozzle as shown in Figures 3c and 3d under same conditions of the above system temperature and pressing forces at 200 000 fs.

These phenomena happen as shown in Figures 2 and 3 are the initial evidences that proves about separated ability of the fluidic Nano-jet to produce the Nano-droplets from the nozzle plate's surface under effecting the various ejective hole diameters which do not depend on the simulation time.

3.2 The Nano-fluidic molecule trajectory and the Nano-droplet production ability

Beside the parameters about the nozzle diameters and simulation time were used to explain for the fluidic Nano-droplet production ability. However, the movement trajectory of the molecules in the ejection process is also

adopted to analyze and explain for the Nano-jet separation ability to produce the fluidic Nano-droplets.

The snapshots as shown in Figure 4 are trajectories of fluidic molecule for 25 and 40-Å-diameter nozzles at 150 000 fs. The pictures show that the fluidic molecules close to the nozzle hole have a lot of confusion movement inside the ejective device with the very zigzag trajectory. However, the molecules had quite straight trajectories after ejecting out through the nozzle. Then they moved away from the nozzle's surface to form the fluidic Nano-jets. While, some molecules which have the low velocity moving sinuously near the nozzle's surface in short time and then tightly adhere on the bottom of the Nano-jets. The cause about the molecular trajectory explains for the reason which the diameter at the Nano-jet bottom is greater than in comparison with other positions of the jet. This is an important cause which affect to the Nano-droplet production ability of the fluidic molecule.

The photos about trajectories of fluidic molecule for 25 and 40-Å-diameter nozzles at 200 000 fs are shown as in Figure 5. The picture 5.a shows that the almost fluidic molecules do not only no move away from the nozzle's surface but also move back towards the nozzle's surface. These molecular trajectories become more curves when increasing the simulation time. On the contrary, the fluidic molecules do not only move away from the nozzle's surface but also become straighter with 40-Å-diameter nozzle as shown in Figure 5b. These molecules continue to go up forming the Nano-jet and then separating to produce the Nano fluidic droplets. This is the reason which is used to explain for affecting of nozzle size to formation ability of Nano-fluidic droplets.

The fluidic molecular density inside the device at each 5 000 femtosecond (fs) instant are shown as in Figure 6. The initial density magnitude without pressing force was
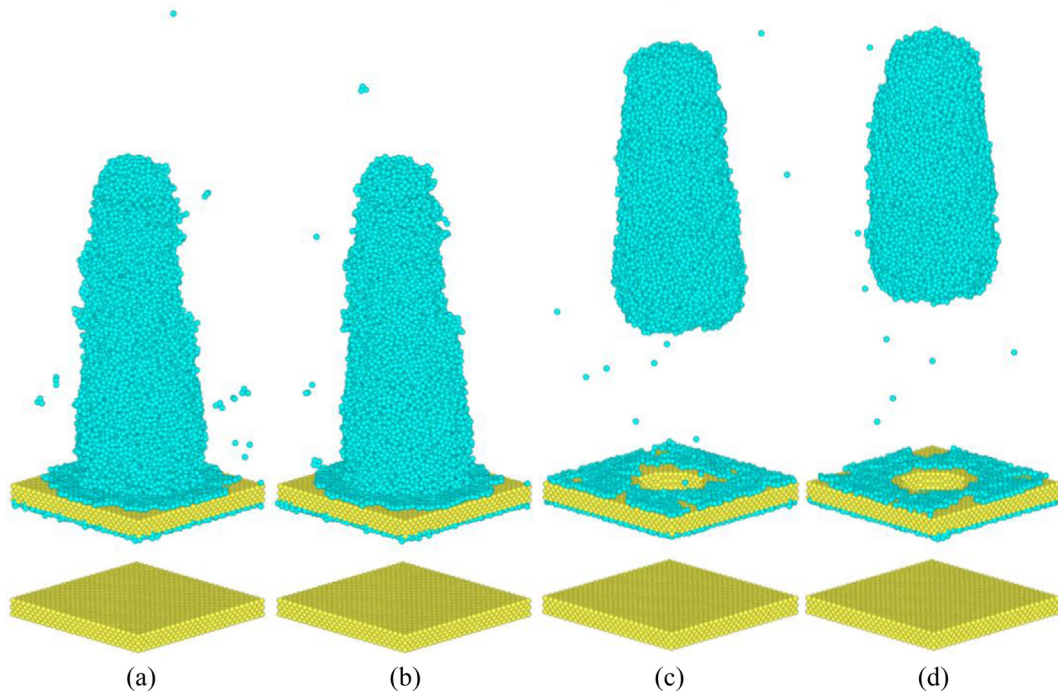
Fig. 3. Snapshots of the fluidic Nano-jet at 200 000 fs: (a) and (b) fluidic Nano-jets of 25-Å-diameter nozzle; (a) and (b) fluidic Nano-jets of 40-Å-diameter nozzle.
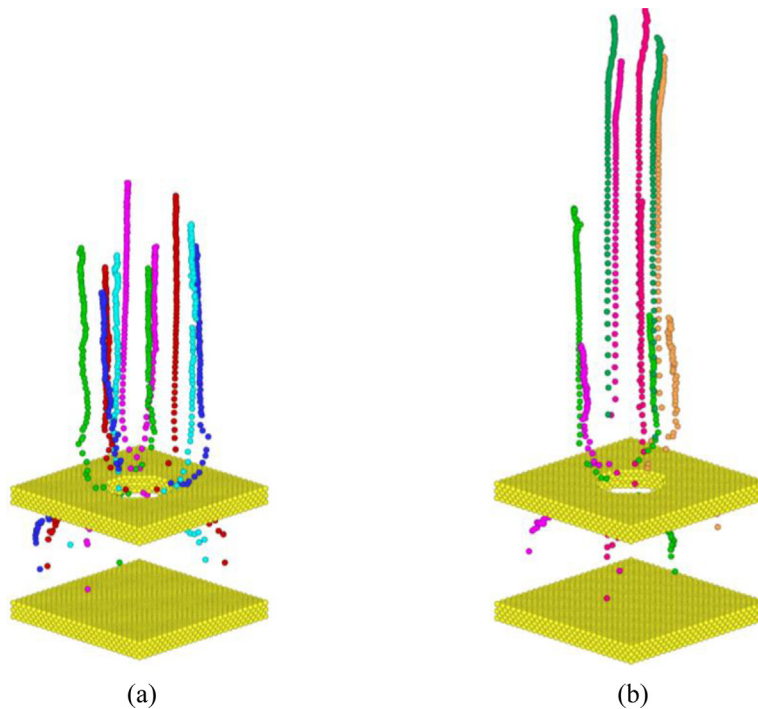

Fig. 4. Trajectories of fluidic molecules at 150 000 fs for 25 and 40-Å-diameter nozzles.

created at $0.37\,\text{g/cm3}$. When the pressing force acts on the device bottom and making the back plate moves upward, the molecular density has the magnitude rapidly increasing at the beginning stage with a wide band for 25-Å-diameter nozzle hole. This quick change is a main cause which has the effect to the continued ejection stream and causes out the necking of the fluidic jet. Simultaneously, this is also a cause which affects to the upward z-direction velocity of the jet. Shortly after, these density magnitudes gradually reach the steady values of 0.75 and 0.69 for the 25-, and 40-Å-diameter nozzle holes, respectively. Intuitively, the time ejects the fluid through the
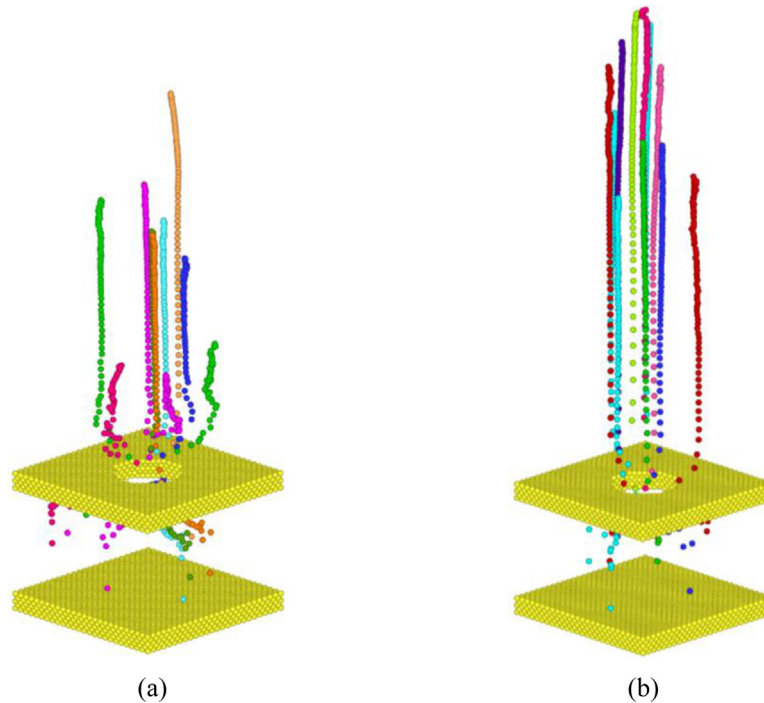
Fig. 5. Trajectories of fluidic molecules at 200 000 fs for 25 and 40-Å-diameter nozzles.
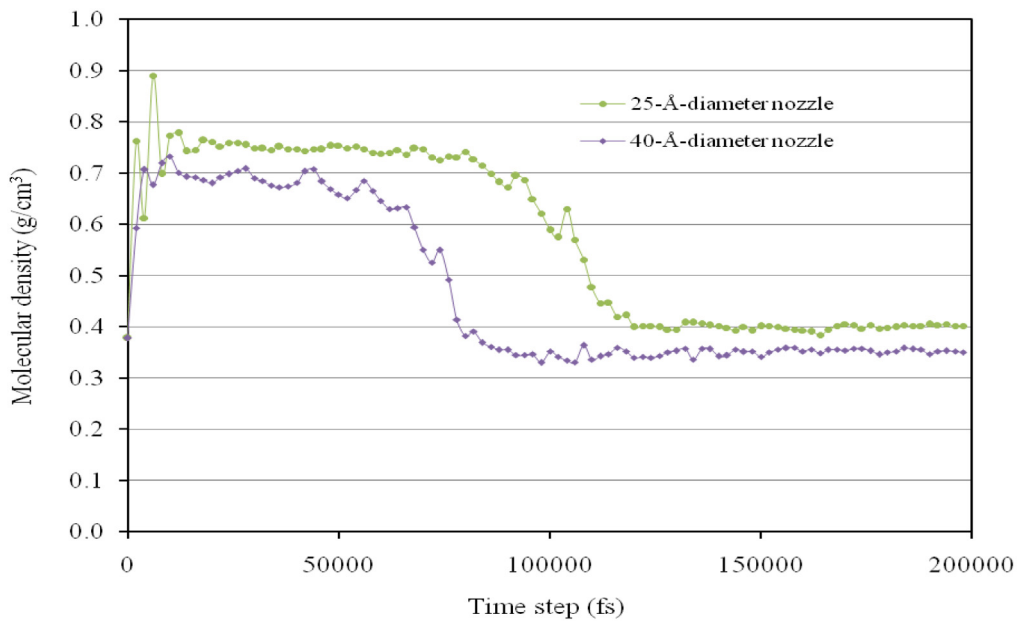

Fig. 6. Diagram of molecular density inside the device at each 5 000 femtosecond instants.

nozzle hole is longer for the hole diameter is smaller. Finally, the molecular density magnitude falls back to approximately the initial density magnitude of 0.37 g/cm3 at the end stage of the molecular ejection process.

In order to investigate the collision of fluidic molecule on the wall of nozzle hole which affect to the molecular ejection trajectory and Nano-droplet production ability after ejecting molecule out of the nozzle hole, the molecular ratio is divided into two groups along the z-direction as shown in Figure 7. The first group is investigated for an annular volume of 2 Å permanent radius which is close to the wall of nozzle hole. The second group is the rest volume for both the 25- and 40-Å-diameter nozzle hole.

The molecular ratio between the two fluidic molecular groups inside the 25- and 40-Å-diameter nozzle hole at each 10 000 fs instant is shown as in Figure 8. There are two change statuses of the molecular ratio during the ejection process through the nozzle hole.
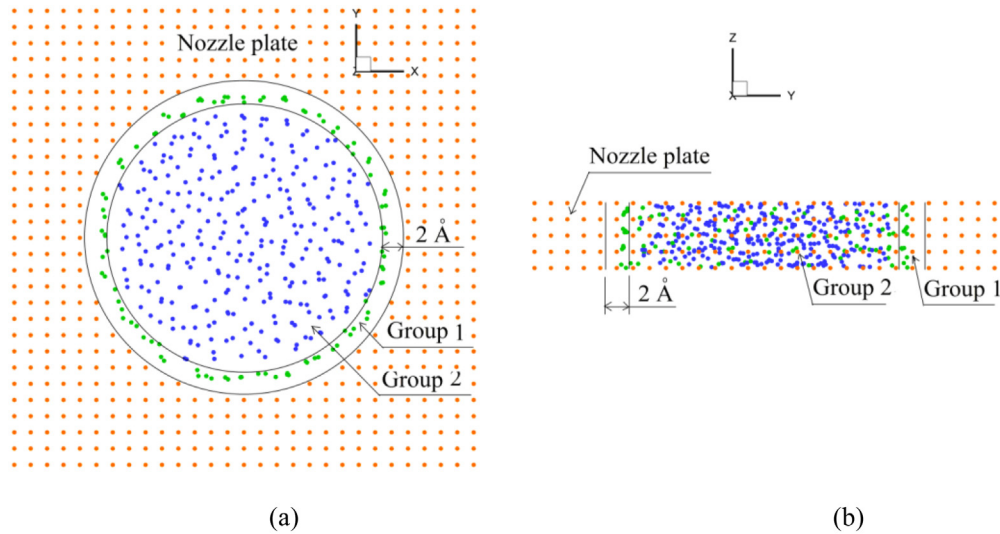
Fig. 7. Two molecular groups inside the nozzle hole volume: (a) View according to the projection from top to bottom of nozzle plate; (b) View according to the vertical projection of nozzle plate.
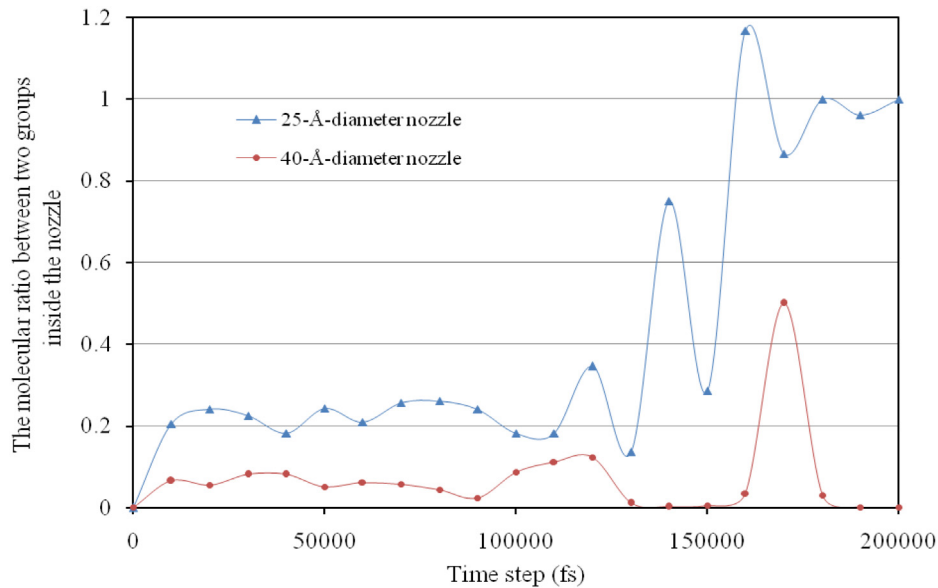

Fig. 8. Diagram of the molecular ratio between two sections inside the nozzle hole.

In the first stage, the ratios both oscillate in the narrow band and increase at the ending stage. The ratio magnitude of 40-Å-diameter nozzle hole is smaller than that of 25-Å-diameter nozzle hole. The ratio magnitude means the molecule have a high density in the annular volume which proves many collisions of molecule on the wall of 25-Å-diameter nozzle. That affects to the molecular velocity value and the Nano-droplet production ability after ejecting molecule out through the nozzle hole.

In the ending stage, almost of the molecule were ejected out through the nozzle hole already, the low velocity molecule which are close to the nozzle' surface dropping back onto the nozzle. The nozzle plate which makes by the gold atoms pulls the fluidic molecule towards the wall of the nozzle hole by the attraction force, thus the fluidic molecular density significantly increases inside nozzle hole at this ending stage.

Figure 9 shows the molecular average velocity according to the x- and y-horizontal directions which close to the wall of the nozzle hole of 2 Å. The velocity magnitude rapidly increases at the initial stage of the molecular ejection process and get to an equilibrium status at 130 000 and 60 000 fs for the 25-, and 40-Å-diameter nozzle holes, respectively. The nozzle hole has a smaller diameter which yields higher velocity magnitude. Thus, molecular ejection direction changes due to the collision molecule on the nozzle wall. The molecule move perpendicular in comparison to the axis of the fluidic molecular Nano-jet.
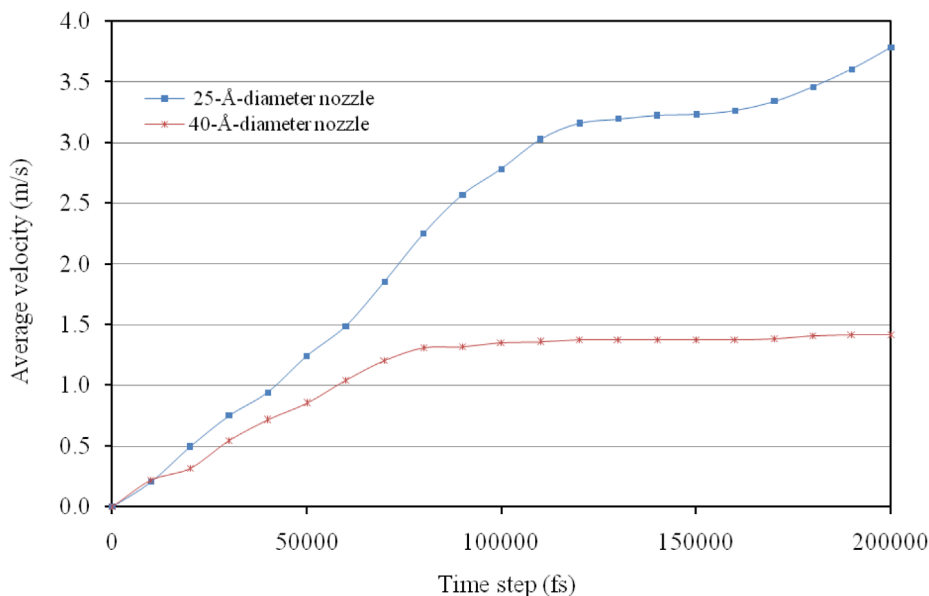
Fig. 9. Diagram of molecular average velocity in x- and y-directions inside the nozzle hole

The Nano-jet has the downward movement after getting the maximum jet height but not separating from the nozzle's surface. That is because the molecules inside the Nano-jet are pulled by the attraction force among the gold atoms and the fluidic molecules on the wall of nozzle hole. This is the main reason which causes increasing at the bottom of fluidic Nano-jet and affects to the Nano-droplet production ability for the smaller nozzle diameter.

4 Conclusions

The molecular dynamics simulation is used in this research to investigate the fluidic molecular trajectory and the Nano-droplet production ability. Based on the above obtained result, the following conclusions are presented out:

The fluidic Nano-droplet production ability is affected by the size of ejective diameter which does not depend on the simulation time and pressing force.

The fluidic molecules close to the nozzle hole have a lot of confusion movement inside the ejective device with the very zigzag trajectory which causes the low molecular velocity moving sinuously trajectory near the nozzle's surface and affects to the Nano-droplet production ability of the fluidic molecule.

The molecular ratio magnitude is smaller than for the larger nozzle diameter which means the molecule has a high density in the annular volume and causes many collisions of molecule on the wall of the smaller nozzle hole. That affects to the molecular velocity value and the Nano-droplet production ability after ejecting molecule out through the nozzle hole.

The molecular average velocity according to the x- and y-horizontal directions which has the position close to the wall of the nozzle hole of 2 Å yields higher velocity magnitudes for the smaller diameter. That is the main reason which causes increasing at the bottom of fluidic Nano-jet and affects to the Nano-droplet production ability for the smaller nozzle diameter.

References

1. Y. Li, J. Xu, D. Li, Microfluid, Nanofluid. **9**, 1011–1031 (2010)
2. Q.N. Van, S.P. Xuan, W.L. Jau, Separation criteria of nanoscale water droplets from a nozzle plate surface, MATEC Web Conf. **169**, 01016 (2018)
3. Y. Li, J.X. Dong, D. Li, Molecular dynamics simulation of nanoscale liquid flows, Microfluid Nanofluid. **9**, 1011–1031 (2010)
4. C. Duan, W. Wang, Q. Xie, Fabrication of nanofluidic devices, Biomicrofluidics **7**, 1932–1058 (2013)
5. A. Dalili, S. Chandra, J. Mostaghimi, Formation of liquid sheets by deposition of droplets on a surface, J. Colloid Interface Sci. **418**, 292–299 (2014)
6. N.S.R. Krishnan, S.P. Uppu, A novel approach for noise prediction using Neural network trained with an efficient optimization technique, Int. J. Simul. Multidisci. Des. Optim. **14**, 3 (2023)
7. T.T.B. Ngo, V.T. Nguyen, T.H. Fang, Nanoscale friction behavior and deformation during copper chemical mechanical polishing process, J. Mol. Model. **29**, 293 (2023)
8. N. Gopan, S.P. Sathian, The role of thermal fluctuations on the formation and stability of nano-scale drops, Colloids Surf. A Physicochem Eng. Asp. **432**, 19–28 (2013)
9. N. Gopan, S.P. Sathian, A langevin dynamics study of nanojets, J. Mol. Liq. **200**, 246–258 (2014)
10. M. Jia, B.Y. Jae, Z. Xuehua, Viscosity-mediated growth and coalescence of surface nanodroplets, J. Phys. Chem. C, **124**, 12476–12484 (2020)
11. J. Zhao, Study on the cylindrical liquid nanojet break-up phenomenon, J. Therm. Sci. **24**, 194–201 (2015)
12. A. Suphanat, Y.M.A. Elisa, Y. Jingjie, Y.N. Teng, Many-body dissipative particle dynamics simulations of nanodroplet formation in 3D nano-inkjet printing, Model. Simul. Mater. Sci. Eng. **27**, (2019)

V.Q. Nguyen et al.: Int. J. Simul. Multidisci. Des. Optim. **15**, 6 (2024)

9

13. Q. Jiasheng, F.A. Gilmar, Z. Xuehua, Surface nanodroplets: formation, dissolution, and applications, Langmuir **35**, 12583–12596 (2019)

14. J. Zhao, Study on the cylindrical liquid nanojet break-up phenomenon, J. Therm. Sci. **24**, 194–201 (2015)

15. J. Huicong, T. Hua, One dimensional model for droplet ejection process in inkjet devices, MDPI ACS Style **28** (2018)

16. Q. Li, Q. Liu, Molecular dynamics simulation of heat transfer with effects of fluid-lattice interactions, Int. J. Heat Mass Transf. **55**, 8088–8092 (2012)

17. D.Wu. Cheng, M.K. Li, J.L. Shiang, H.F. Te, Effects of temperature, size of water droplets, and surface roughness, Comput. Mater. Sci. **53**, 25–30 (2012)

18. T. Ramesh, A.S. Praveen, P.B. Pillai, Numerical simulation of heat sinks with different configurations for high power LED thermal management, Int. J. Simul. Multidisci. Des. Optim. **13**, 18 (2022)

19. Q.N. Van, W.L. Jau, Investigation of temperature effects on nanoscale water droplet separation onto a fixed solid plate, Simulation: Transactions of the Society for Modeling and Simulation International. 1–9 (2016)

20. Q.N. Van, T.N. Van, D.H. Tien, Investigating the influential factors of ejective time and compressible force magnitude to fluid jet movement, Int. J. Simul. Multidisci. Des. Optim. **12**, 1–3 (2021)

21. M. Levitt, M. Hirshberg, R. Sharon, K.E. Laidig, V. Daggett, Calibration and testing of a water model for simulation of the molecular dynamics of proteins and nucleic acids in solution, J. Phys. Chem. B, **101**, 5051–5061 (1997)